Modeling the coronary artery tree

Cristian Lorenz, Jens von Berg, Thomas Bülow, Steffen Renisch, Sven Wergandt

***Abstract*—The paper describes a model of the coronary artery tree. It has been developed for the context of medical image processing and medical reporting. The model combines geometric information with associated medical nomenclature and anatomical relations. Applicability of the model and inter-individual geometrical variability has been studied by matching the model to the individual coronary anatomy of 33 patients imaged with a multi-detector-row computer tomography scanner.**

***Index Terms*—anatomical modeling, coronary model, medical image processing.**

I. Introduction

Coronary arteries are a key subject in cardiac diagnosis and therapy. Several medical imaging modalities such as X-ray, computer tomography, and magnetic resonance imaging are available to assess the condition of the coronary vasculature. Applying domain knowledge in the form of a coronary artery model can considerably enhance associated algorithms for medical image processing, visualization, and reporting.

II. Model content

A. Geometry

With respect to image processing tasks such as the segmentation of the coronary arteries (see e.g. [3]), an estimate of the expected course of the coronary arteries within the imaged anatomy is of large interest. This information can for example help to bridge gaps caused by either imaging errors (e.g. motion artifacts) or by true vascular properties (e.g. a stenosis). We base the geometry content of our model on the results of Dodge et al. [1] who extracted a mean end-diastolic model of the coronary centerlines from bi-planar coronary angiography images of 37 patients. In a further publication, Dodge reports also the diameter of the main coronary arteries [2]. Based on point-sets of Dodge et al. we construct a tree-model of the coronary centerlines represented as points-sets connected by linear line segments. Alternatively, the point-sets can be connected by e.g. cubic splines.

B. Anatomical Nomenclature

Combining the pure geometrical information with the cardiac nomenclature as commonly used in the clinical context enables adequate and efficient user interaction functionality, such as an annotated display of results, manual identification of structures, correction of results etc. We used the terms and the schematic view as defined in [5] as source for the nomenclature related model content. Especially the “active” schematic view (see Fig. 2) is an efficient means for user interaction. Depending on the context mode, the user may select sub-structures of the coronary artery tree for further processing, or a segmentation algorithm feeds back results about found or missing structures.

C. Anatomical Relations

Anatomical relations, such as “is-part-of”, “is-inside-of”, “is-distal-of”, etc. play a crucial role for supporting anatomical reasoning during an image-processing task. It is a frequent problem during the segmentation of the coronary arteries to distinguish between structures that have been incorrectly identified as a coronary artery and true coronary arteries. In addition, anatomical relations facilitate user interaction and navigation in the coronary tree. Within the adaptation study described below, the “is-part-of” relation has been used to exclude anatomically impossible data-to-model matches during the optimization.

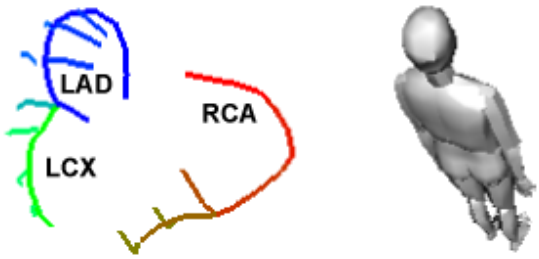

Fig. 1. End-diastolic coronary centerlines. Blue: Left anterior descending coronary artery and branches, green: Circumflex artery and branches, red: right coronary artery and branches. The manikin at the right hand side depicts the viewing geometry.

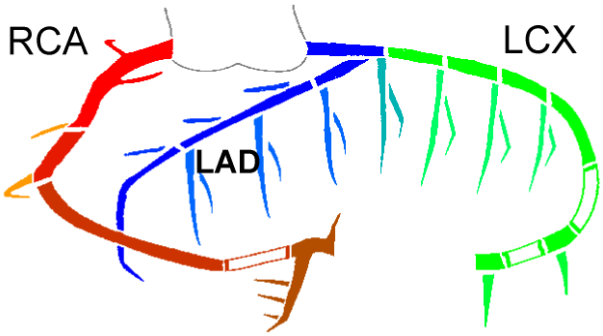

Fig. 2. Schematic view of the coronary artery system as used by the American Heart Association [5].

All authors are with the Philips Research Laboratory Hamburg, D-22335 Hamburg, Röntgenstrasse 24-26, (phone: +49-40-5078-2063, fax: +49-40-5078-2510, email: Cristian.Lorenz@Philips.com)

III. PATIENT DATA

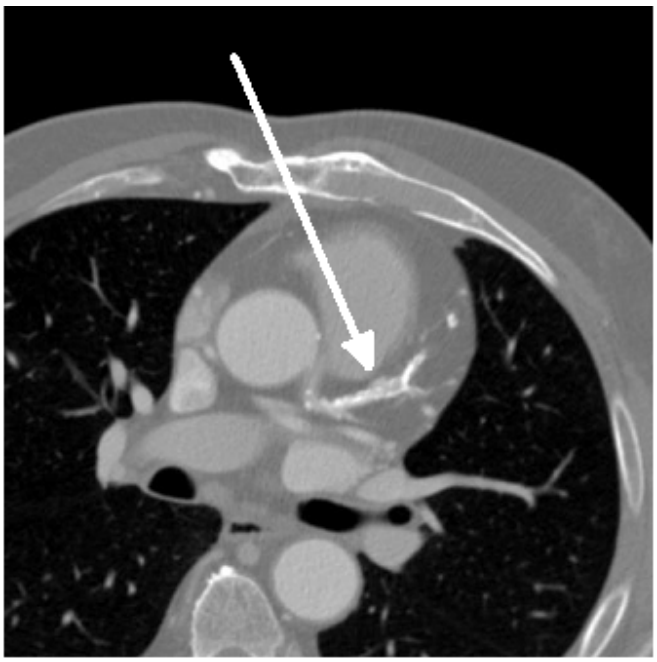

Fig 3. Axial slice of a multi-detector-row CT angiography scan. The arrow indicates a portion of left anterior descending coronary artery. The bright portions indicate calcifications.

In order to verify the geometric content of the model described above, the model has been matched to a set of 33 individual coronary centerlines that have been extracted from cardiac multi-detector-row CT angiographic images (see e.g. [8] and Fig. 3). The number and length of visible coronary artery segments differs largely in the set of patient data; therefore we restricted the analysis to the three main coronary arteries (RCA=right coronary artery, LAD=left anterior descending coronary artery, and LCX=circumflex coronary artery) in order to achieve a common set of structures (see Table 1). For all patients the centerlines of the three main coronary arteries have been manually delineated and anatomically annotated. The centerlines have been re-sampled with a fixed point distance of 2 mm.

IV. MODEL ADAPTAION

The model was adapted to the patient data minimizing the Euclidean distances between data-points and model lines. The adaptation is performed in three steps, adding successively additional degrees of freedom (DOF) to the transformation of the 3D point coordinates of the centerline model. In a first step, the model deformation is restricted to a rigid transformation (6 DOF), allowing only translation and rotation. In a second step, an overall scaling is added leading to a similarity transform (7 DOF) and in a third step, a general affine transformation is applied, allowing rotation, scaling and shear (12 DOF). The shear component of the affine transformation can be interpreted as an an-isotropic scaling in arbitrary direction.

In each step, the parameters are simultaneously optimized in a down-hill simplex (or polytope) optimization procedure [6,9]. In this scheme, for an n-dimensional optimization problem n+1 parameter vectors are maintained (the simplex) which span a sub-volume in the parameter space. During the optimization the simplex moves through the parameter space, mainly by changing the position of the worst vertex. The optimization is stopped if a certain fractional convergence tolerance is reached. The fractional convergence tolerance δ evaluates the difference between the best (lowest) and worst (highest) objective function value f for the current simplex and is defined as:

$$\delta = 2\frac{|f_{best} - f_{worst}|}{|f_{best}| + |f_{worst}|}.$$

The objective function being minimized evaluates the distances between data-points and model lines. For each data point the shortest distance to the anatomically corresponding model-line is determined. The objective function sums the squared distance values for all data-points.

The optimization starts with an initial simplex of n+1 parameter vectors. The first parameter vector resembles an identity transform for the rotational (or linear, if affine) transformation part and a translation vector that moves the model center to the center of the data-lines (Fig. 4a). The remaining n parameter vectors are derived from the first one by adding a slight variation to each of the n parameters, i.e. parameter vector 1+i is derived from the first parameter vector by adding a variation to the i-th parameter.

Length (mm)	LAD Instances	LCX Instances	RCA Instances
20		2	
30		3	1
40		5	1
50		3	0
60	2	4	1
70	3	5	4
80	1	5	2
90	2	4	2
100	2	2	4
110	2		2
120	5		6
130	3		5
140	3		2
150	2		2
160	2		1
170	3		
180	3		

Table 1: Histogram of the length of the three main coronary arteries that could be delineated in 33 patient data sets.
Length of the coronaries in the coronary model :
Left dominance: LAD:168 mm, LCX:99 mm, RCA:103 mm
Right dominance: LAD:168 mm, LCX:77 mm, RCA:215 mm

Transformation type	Mean residual distance	Maximal residual distance	Standard deviation
Rigid	6.3 mm	31.9 mm	3.8 mm
Similarity	5.4 mm	25.9 mm	3.3 mm
Affine	2.7 mm	16.0 mm	2.0 mm

Table 2: Adaptation result for the three transformation types applied to coronary centerlines from 33 patients (total number of data-points: 5048).

V. RESULTS

The optimization scheme described above has been applied to match the extracted centerlines from 33 patients. The optimization was started with an initial simplex generated with a parameter variation of 0.05 for the linear transformation part (corresponds to about 4 degrees rotation) and 2.0 mm for the translation part. The optimization was stopped when a fractional convergence tolerance of $\delta = 10^{-10}$ has been reached.

Fig. 4 shows data and model lines after initial translation (Fig. 4a) and after optimization of the rigid (Fig. 4b) and affine (Fig. 4c) coordinate transformation. In total the 33 patient derived coronary centerlines consisted of 5048 points (sampled with 2 mm distance). A histogram of the residual data-to-model distances after optimization shows Fig. 5. The mean residual distances after optimization are shown in Table 2. Figure 5 and Table 2 show that reasonable match between the coronary model and patient derived data can be achieved already by a comparably inflexible global affine transformation. The mean residual distance after an optimal affine transformation is half of the mean residual distance after an optimal similarity transformation. Figures 6 and 7 show a histogram of resulting rotation and scaling respectively. We express the 3D rotation by a unit vector defining the axis of rotation (2 DOF) and a rotation angle (1 DOF), the latter is plotted in Fig. 6. The large rotation angles up to 45 degrees are consistent with clinical findings showing the large variability of the long-axis direction of the heart.

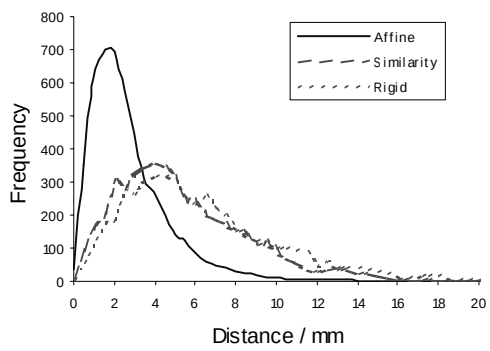

Fig. 5: Histogram of the residual data-point to model line distances after optimization.

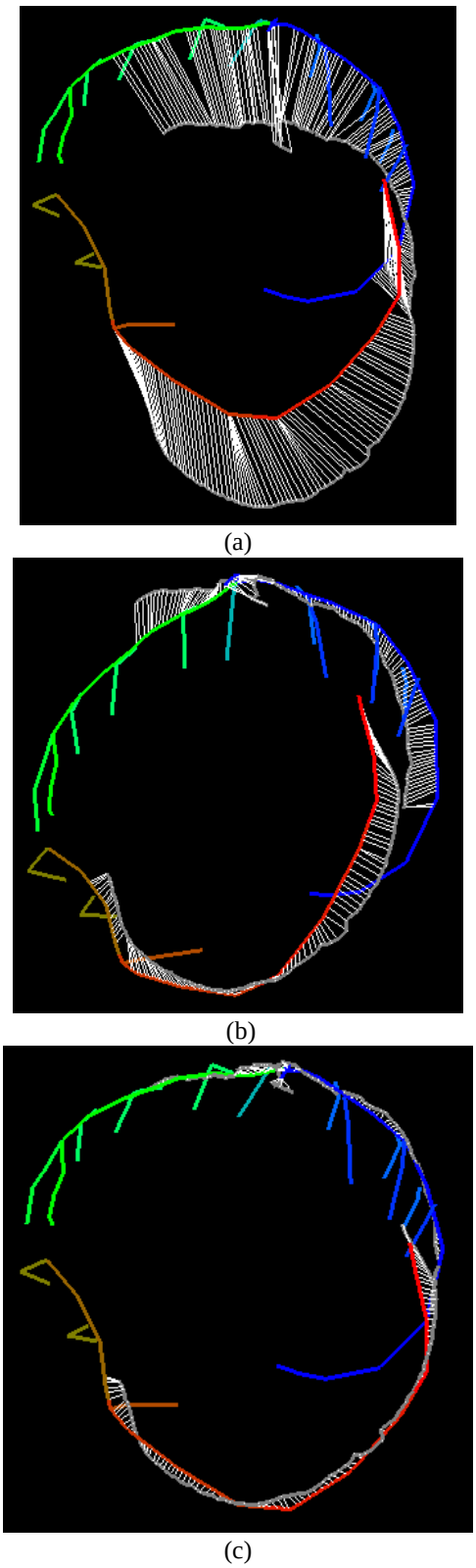

(a) (b) (c)

Fig. 4: Model (colored), the data centerlines (gray) and the data-point to model line correspondence (thin dark-gray lines) after (a) translating the model center to the center of the data lines and (b) rigid adaptation (c) affine adaptation.

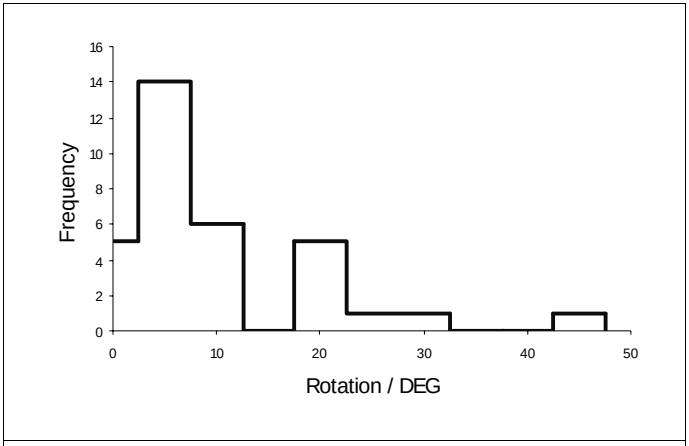

Fig. 6: Histogram of the model rotation angle after model adaptation using a rigid transformation (translation, rotation).

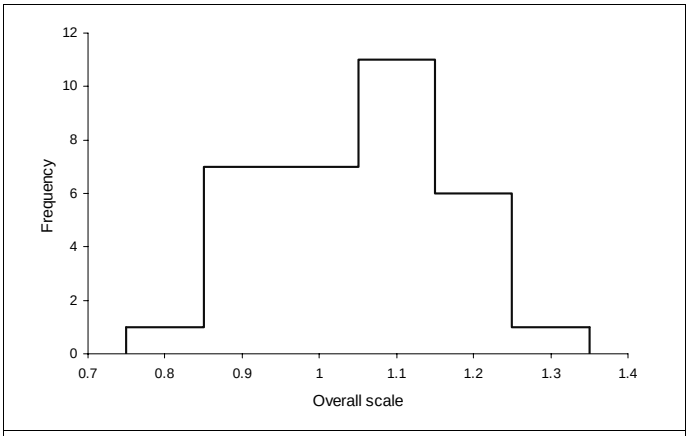

Fig. 7: Histogram of the overall model scale after model adaptation using a similarity transformation (translation, rotation and uniform scale).

VI. Conclusion

It could be verified, that an end-diastolic coronary artery model can be adapted to patient data containing the three main coronary arteries with an accuracy of a few mm. The procedure can be used during the segmentation of the coronary arteries, e.g. for the detection of missing parts of the coronary tree and as guidance during the search for coronary segments. The procedure is also an important step towards the generation of an improved coronary model, being based on an enlarged set of learning samples. By using the inverse of the transformations resulting from the model-to-data adaptation, all patient derived centerlines can be transformed into the model coordinate system in order to establish inter-data point correspondence. This is necessary for the generation of a statistical model, being based on a learning set of corresponding parameter vectors.

Based on multi-phase cardiac computer tomography data, we intend to use the described method for assessing to which degree the temporal variability of the coronary arteries during the heart beat can be described by an affine transformation.

Acknowledgment

We thank Philips Medical Systems Cleveland, for providing the multi-detector-row CT image data and especially P. C. Johnson for providing a part of the patient derived coronary centerlines.

References

[1] J.T. Dodge, B.G. Brown, E.L. Bolson, and H.T. Dodge, Intrathoracic spatial location of specified coronary segments on the normal human heart. Applications in quantitative arteriography, assessment of regional risk and contraction, and anatomic display Circulation 78: p. 1167-1180, 1988

[2] J.T. Dodge, B.G. Brown, E.L. Bolson, and H.T. Dodge, Lumen diameter of normal human coronary arteries. Influence of age, sex, anatomic variation, and left ventricular hypertrophy or dilation, Circulation 86: p. 232-246, 1992 H. Poor, *An Introduction to Signal Detection and Estimation*. New York: Springer-Verlag, 1985, ch. 4.

[3] C. Lorenz, S. Renisch, S. Schlathölter, T. Bülow, SPIE, Simultaneous Segmentation and Tree Reconstruction of the Coronary Arteries in MSCT Images, Int. Symposium Medical Imaging, 15-20 Feb. 2003, San Diego, Proc. SPIE Vol. 5032, p. 167-177

[4] D. Sherknies, J. Meunier, A numerical 3D coronary tree model, in Proceedings of the 16th Congress of Computer assisted radiology and surgery (CARS 2002), Springer, p. 814-818, 2002

[5] P.J. Scanlon, D.P. Faxon, ACC/AHA Guidelines for Coronary Angiography, Journal of the American College of Cardiology, Vol. 33, No. 6, 1999, p. 1756-1824

[6] W.H. Press, S. A. Teukolsky, W.T. Vetterling, B.P. Flannery, Numerical Recipes in C, Cambridge Univ. Press1992, Chapter 10.4

[7] G.H. Golub, C.F. van Loan, Matrix Computations, Johns Hopkins University Press, Baltimore, 1996, Chapter 4.2.10

[8] Z.A. Fayad, V. Fuster, K. Nikolaou, C. Becker, Computed Tomography and Magnetic Resonance Imaging for Noninvasive Coronary Angiography and Plaque Imaging: Current and Potential Future Concepts, Circulation, Oct 2002; 106: 2026 - 2034.

[9] P. E. Gill, W. Murray, M. H. Wright, Practical Optimization, Academic Press, San Diego, 1997, Chapter 4.2.2

[10] S. Wergandt, Modelling the coronary arteries of the human heart, Diploma thesis, University Stuttgart, May 20, 2003